CORRESPONDENCE

Aerosol and Surface Stability of SARS-CoV-2 as Compared with SARS-CoV-1

TO THE EDITOR: A novel human coronavirus that is now named severe acute respiratory syndrome coronavirus 2 (SARS-CoV-2) (formerly called HCoV-19) emerged in Wuhan, China, in late 2019 and is now causing a pandemic.[1] We analyzed the aerosol and surface stability of SARS-CoV-2 and compared it with SARS-CoV-1, the most closely related human coronavirus.[2]

We evaluated the stability of SARS-CoV-2 and SARS-CoV-1 in aerosols and on various surfaces and estimated their decay rates using a Bayesian regression model (see the Methods section in the Supplementary Appendix, available with the full text of this letter at NEJM.org). SARS-CoV-2 nCoV-WA1-2020 (MN985325.1) and SARS-CoV-1 Tor2 (AY274119.3) were the strains used. Aerosols (<5 μm) containing SARS-CoV-2 ($10^{5.25}$ 50% tissue-culture infectious dose [$TCID_{50}$] per milliliter) or SARS-CoV-1 ($10^{6.75-7.00}$ $TCID_{50}$ per milliliter) were generated with the use of a three-jet Collison nebulizer and fed into a Goldberg drum to create an aerosolized environment. The inoculum resulted in cycle-threshold values between 20 and 22, similar to those observed in samples obtained from the upper and lower respiratory tract in humans.

Our data consisted of 10 experimental conditions involving two viruses (SARS-CoV-2 and SARS-CoV-1) in five environmental conditions (aerosols, plastic, stainless steel, copper, and cardboard). All experimental measurements are reported as means across three replicates.

SARS-CoV-2 remained viable in aerosols throughout the duration of our experiment (3 hours), with a reduction in infectious titer from $10^{3.5}$ to $10^{2.7}$ $TCID_{50}$ per liter of air. This reduction was similar to that observed with SARS-CoV-1, from $10^{4.3}$ to $10^{3.5}$ $TCID_{50}$ per milliliter (Fig. 1A).

SARS-CoV-2 was more stable on plastic and stainless steel than on copper and cardboard, and viable virus was detected up to 72 hours after application to these surfaces (Fig. 1A), although the virus titer was greatly reduced (from $10^{3.7}$ to $10^{0.6}$ $TCID_{50}$ per milliliter of medium after 72 hours on plastic and from $10^{3.7}$ to $10^{0.6}$ $TCID_{50}$ per milliliter after 48 hours on stainless steel). The stability kinetics of SARS-CoV-1 were similar (from $10^{3.4}$ to $10^{0.7}$ $TCID_{50}$ per milliliter after 72 hours on plastic and from $10^{3.6}$ to $10^{0.6}$ $TCID_{50}$ per milliliter after 48 hours on stainless steel). On copper, no viable SARS-CoV-2 was measured after 4 hours and no viable SARS-CoV-1 was measured after 8 hours. On cardboard, no viable SARS-CoV-2 was measured after 24 hours and no viable SARS-CoV-1 was measured after 8 hours (Fig. 1A).

THIS WEEK'S LETTERS

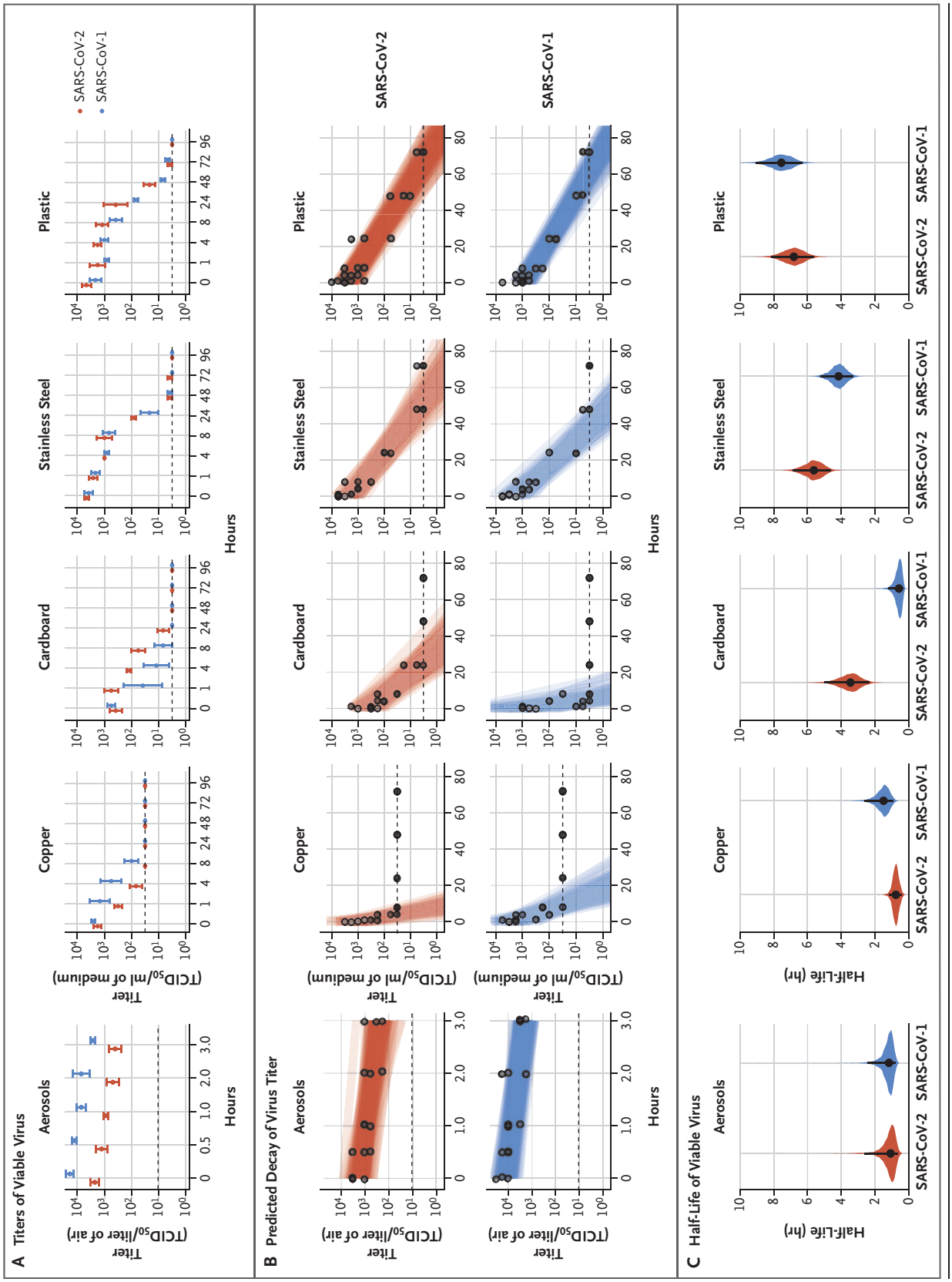

Figure 1 (previous page). Viability of SARS-CoV-1 and SARS-CoV-2 in Aerosols and on Various Surfaces.

As shown in Panel A, the titer of aerosolized viable virus is expressed in 50% tissue-culture infectious dose ($TCID_{50}$) per liter of air. Viruses were applied to copper, cardboard, stainless steel, and plastic maintained at 21 to 23°C and 40% relative humidity over 7 days. The titer of viable virus is expressed as $TCID_{50}$ per milliliter of collection medium. All samples were quantified by end-point titration on Vero E6 cells. Plots show the means and standard errors (I bars) across three replicates. As shown in Panel B, regression plots indicate the predicted decay of virus titer over time; the titer is plotted on a logarithmic scale. Points show measured titers and are slightly jittered (i.e., their horizontal positions are modified by a small random amount to reduce overlap) along the time axis to avoid overplotting. Lines are random draws from the joint posterior distribution of the exponential decay rate (negative of the slope) and intercept (initial virus titer) to show the range of possible decay patterns for each experimental condition. There were 150 lines per panel, including 50 lines from each plotted replicate. As shown in Panel C, violin plots indicate posterior distribution for the half-life of viable virus based on the estimated exponential decay rates of the virus titer. The dots indicate the posterior median estimates, and the black lines indicate a 95% credible interval. Experimental conditions are ordered according to the posterior median half-life of SARS-CoV-2. The dashed lines indicate the limit of detection, which was $3.33\times10^{0.5}$ $TCID_{50}$ per liter of air for aerosols, $10^{0.5}$ $TCID_{50}$ per milliliter of medium for plastic, steel, and cardboard, and $10^{1.5}$ $TCID_{50}$ per milliliter of medium for copper.

Both viruses had an exponential decay in virus titer across all experimental conditions, as indicated by a linear decrease in the $\log_{10}TCID_{50}$ per liter of air or milliliter of medium over time (Fig. 1B). The half-lives of SARS-CoV-2 and SARS-CoV-1 were similar in aerosols, with median estimates of approximately 1.1 to 1.2 hours and 95% credible intervals of 0.64 to 2.64 for SARS-CoV-2 and 0.78 to 2.43 for SARS-CoV-1 (Fig. 1C, and Table S1 in the Supplementary Appendix). The half-lives of the two viruses were also similar on copper. On cardboard, the half-life of SARS-CoV-2 was longer than that of SARS-CoV-1. The longest viability of both viruses was on stainless steel and plastic; the estimated median half-life of SARS-CoV-2 was approximately 5.6 hours on stainless steel and 6.8 hours on plastic (Fig. 1C). Estimated differences in the half-lives of the two viruses were small except for those on cardboard (Fig. 1C). Individual replicate data were noticeably "noisier" (i.e., there was more variation in the experiment, resulting in a larger standard error) for cardboard than for other surfaces (Fig. S1 through S5), so we advise caution in interpreting this result.

We found that the stability of SARS-CoV-2 was similar to that of SARS-CoV-1 under the experimental circumstances tested. This indicates that differences in the epidemiologic characteristics of these viruses probably arise from other factors, including high viral loads in the upper respiratory tract and the potential for persons infected with SARS-CoV-2 to shed and transmit the virus while asymptomatic.[3,4] Our results indicate that aerosol and fomite transmission of SARS-CoV-2 is plausible, since the virus can remain viable and infectious in aerosols for hours and on surfaces up to days (depending on the inoculum shed). These findings echo those with SARS-CoV-1, in which these forms of transmission were associated with nosocomial spread and super-spreading events,[5] and they provide information for pandemic mitigation efforts.

Neeltje van Doremalen, Ph.D.
Trenton Bushmaker, B.Sc.
National Institute of Allergy and Infectious Diseases
Hamilton, MT

Dylan H. Morris, M.Phil.
Princeton University
Princeton, NJ

Myndi G. Holbrook, B.Sc.
National Institute of Allergy and Infectious Diseases
Hamilton, MT

Amandine Gamble, Ph.D.
University of California, Los Angeles
Los Angeles, CA

Brandi N. Williamson, M.P.H.
National Institute of Allergy and Infectious Diseases
Hamilton, MT

Azaibi Tamin, Ph.D.
Jennifer L. Harcourt, Ph.D.
Natalie J. Thornburg, Ph.D.
Susan I. Gerber, M.D.
Centers for Disease Control and Prevention
Atlanta, GA

James O. Lloyd-Smith, Ph.D.
University of California, Los Angeles
Los Angeles, CA
Bethesda, MD

Emmie de Wit, Ph.D.
Vincent J. Munster, Ph.D.
National Institute of Allergy and Infectious Diseases
Hamilton, MT
vincent.munster@nih.gov

Dr. van Doremalen, Mr. Bushmaker, and Mr. Morris contributed equally to this letter.

The findings and conclusions in this letter are those of the authors and do not necessarily represent the official position of the Centers for Disease Control and Prevention (CDC). Names of specific vendors, manufacturers, or products are included for public health and informational purposes; inclusion does not imply endorsement of the vendors, manufacturers, or products by the CDC or the Department of Health and Human Services.

Supported by the Intramural Research Program of the National Institute of Allergy and Infectious Diseases, National Institutes of Health, and by contracts from the Defense Advanced Research Projects Agency (DARPA PREEMPT No. D18AC00031, to Drs. Lloyd-Smith and Gamble), from the National Science Foundation (DEB-1557022, to Dr. Lloyd-Smith), and from the Strategic Environmental Research and Development Program of the Department of Defense (SERDP, RC-2635, to Dr. Lloyd-Smith).

Disclosure forms provided by the authors are available with the full text of this letter at NEJM.org.

This letter was published on March 17, 2020, at NEJM.org.

1. Coronavirus disease (COVID-2019) situation reports. Geneva: World Health Organization, 2020 (https://www.who.int/emergencies/diseases/novel-coronavirus-2019/situation-reports/).
2. Wu A, Peng Y, Huang B, et al. Genome composition and divergence of the novel coronavirus (2019-nCoV) originating in China. Cell Host Microbe 2020;27:325-8.
3. Bai Y, Yao L, Wei T, et al. Presumed asymptomatic carrier transmission of COVID-19. JAMA 2020 February 21 (Epub ahead of print).
4. Zou L, Ruan F, Huang M, et al. SARS-CoV-2 viral load in upper respiratory specimens of infected patients. N Engl J Med 2020;382:1177-9.
5. Chen YC, Huang LM, Chan CC, et al. SARS in hospital emergency room. Emerg Infect Dis 2004;10:782-8.

DOI: 10.1056/NEJMc2004973

Epidemiologic and Survival Trends in Amyloidosis, 1987–2019

TO THE EDITOR: Amyloidosis is a group of rare disorders caused by deposition of misfolded proteins as insoluble fibrils, which leads to progressive multiorgan failure and death.[1] The past 30 years have seen remarkable advances in diagnostic imaging, more accurate identification of fibrils, and (in recent years) the first approved treatments.[2,3]

We report here data on 11,006 patients who received a diagnosis of amyloidosis during the period from 1987 through October 2019. All data were obtained from the United Kingdom National Amyloidosis Centre database. The number of cases increased by 670% from the period 1987–1999 to the period 2010–2019 (Fig. 1A). Systemic light-chain (AL) amyloidosis remained the most common type and accounted for 55% of all cases (Fig. 1B). With the advances in therapies that target plasma cells, overall survival among patients with AL amyloidosis increased from a median of 18 months among patients who received a diagnosis before 2005 to

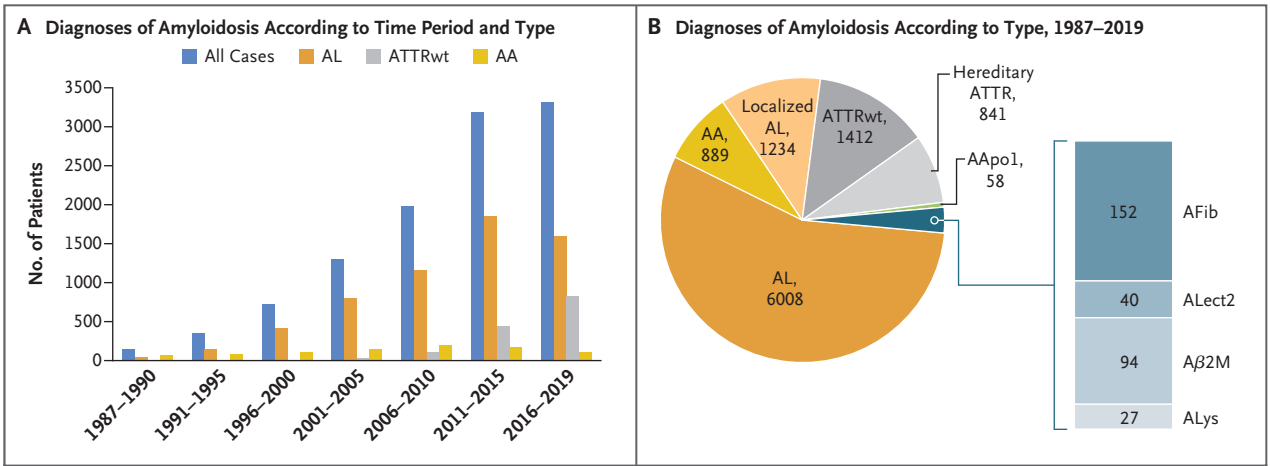

Figure 1. Diagnoses of Amyloidosis over Three Decades and Amyloidosis Types.

Panel A shows data for 11,006 cases of amyloidosis diagnosed from 1987 to 2019. Panel B shows data for the 10,755 cases for which fibril type could be determined accurately. AA denotes amyloid A, AApo1 amyloid apolipoprotein A-I, Aβ2M amyloid beta$_2$-microglobulin, AFib amyloid fibrinogen, ALect2 amyloid leukocyte chemotactic factor 2, AL light chain, ALys amyloid lysozyme, ATTR transthyretin-associated, and ATTRwt wild-type ATTR.